TOPICAL REVIEW — Amorphous physics and materials

Interstitialcy theory of condensed matter states and its application to non-crystalline metallic materials*

V A Khonik†

Department of General Physics, State Pedagogical University, Voronezh 394043, *Russia*

(Received 31 August 2016; revised manuscript received 6 October 2016; published online 22 December 2016)

A comprehensive review of a novel promising framework for the understanding of non-crystalline metallic materials, i.e., interstitialcy theory of condensed matter states (ITCM), is presented. The background of the ITCM and its basic results for equilibrium/supercooled liquids and glasses are given. It is emphasized that the ITCM provides a new consistent, clear, and testable approach, which uncovers the generic relationship between the properties of the maternal crystal, equilibrium/supercooled liquid and glass obtained by melt quenching.

Keywords: liquids and glasses, interstitialcy theory, shear modulus, relaxation

PACS: 64.70.pe, 61.72.jj, 62.20.de **DOI:** 10.1088/1674-1056/26/1/016401

1. Introduction

Non-crystalline materials, liquids and glasses, constitute a subject of unabated interest despite extensive decades-long research. On the one hand, this is due to the fact that these materials play a crucial role in the technological development of mankind. On the other hand, because of the absence of structural periodicity, the non-crystalline state is much more complicated to understand and describe than the crystalline state. Nonetheless, impressive progress has been achieved in this field as discussed in numerous books and reviews, e.g., Refs. [1]–[10]. Amongst other non-crystalline materials, metallic liquids and glasses stay somewhat separately due to their non-directional metallic atomic bonding. Although quite a few well developed basic physical concepts (e.g., on glass formation, relaxation, crystallization, etc.) are applicable to all (or many) types of liquids and glasses (oxide, elemental, semiconductor, chalcogenide, fluoride, metallic, etc.), the specific structural nature of metallic materials often requires developments of particular physical notions. Thus, non-crystalline metallic materials constitute clearly a separate research field. Solid non-crystalline metallic materials, i.e., metallic glasses, have become a hot topic here. Numerous detailed reviews addressing the progress in different research directions related to metallic glasses can be found elsewhere.[11–23]

Despite this progress, certain general unsolved problems in the physics of non-crystalline metallic materials can be outlined, e.g., Refs. [14], [17], [18], [24] and [25]. These issues, to some extent, apply to all solid non-crystalline materials. In particular, it seems to be clear that if solid glass is prepared by quenching the melt while the latter is obtained by melting the maternal crystal, one should expect a generic relation between the physical properties of glass and those of the maternal crystal, which should be considered as a reference structural state. Current literature does not give any route to tracing this relation. It might be possible that this relation can be mediated by the interconnection of defect subsystems of crystal, melt and solid glass. It is this idea that is implied by the Interstitialcy theory of condensed matter states proposed by Granato in 1992 and called ITCM hereafter. It has been found that the ITCM provides clear, comprehensive, and testable explanations of general structural evolution and relevant property change during crystal→melt→glass transformation by using the same ideological approach and giving a solid basis as well as a fully new promising insight into the understanding of glass physical properties. Since 1992, quite a few important results within the framework of the ITCM have been obtained. This theory is reviewed in the present paper. First of all, the ITCM background is to be considered. This background is essentially related to the understanding of point defects in crystals.

2. Background

2.1. Equilibrium point defects in monoatomic crystals

It was suggested by Frenkel[26–28] and now is generally accepted that the only point defects produced by thermal activation in monoatomic crystals are vacancies and interstitials. While vacancies (Frenkel's "holes") are intuitively rather simple to understand, the atomic structure of interstitials was highly debated until the beginning of the 70 s of the past century.[29,30] Before this time, it had been assumed that interstitials occupy the octahedral cavity in the FCC structure (i.e., in the center of the elementary cell). However, Seitz[31]

*Project supported by the Ministry of Education and Science of the Russian Federation (Grant No. 3.114.2014/K).

†Corresponding author. E-mail: khonik@vspu.ac.ru

© 2017 Chinese Physical Society and IOP Publishing Ltd

considered in 1950 "an interstitial atom which moves by jumping into a normal lattice site and forces the atom that is there into a neighboring interstitial site" and called it an "interstitialcy". In the 60s of the past century, Gibson *et al.*[32] and Erginsoy *et al.*[33] performed extended computer simulation of radiation damages of FCC and BCC metallic crystals and concluded that interstitials "reside in a split configuration, sharing a lattice site with another atom". In the middle of the 70s it became clear that interstitial atoms in simple metallic crystals have split dumbbell configuration,[34,35] which is equivalent to Seitz's interstitialcy. It is now commonly accepted that split interstitials exist in all basic crystalline structures and represent the basic state of interstitials in metals. There are numerous theoretical, computational, and experimental evidences for this.[36–42] Examples of these defects in FCC, BCC, and HCP structures are given in Fig. 1. It is seen that all dumbbell (split) configurations consist of two atoms sharing the same lattice site.

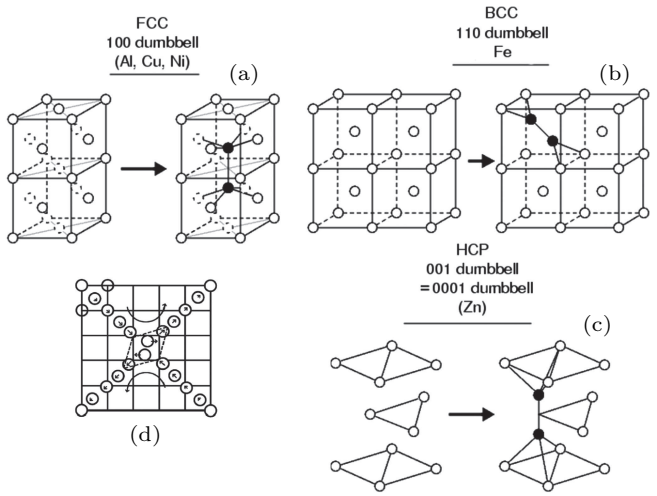


Fig. 1. Dumbbell split interstitials (interstialcies) in different crystalline structures (a)–(c).[34,35] (d) Schematic representation of string-like motion around the intersrtitialcy.[43]

The dumbbell nature of the interstitial defect has far-reaching consequences. First of all, this concerns its formation entropy S_i. Up to the middle of the 70s and even later it was assumed that S_i is rather negative,[30,44] in contrast to the positive formation entropy of vacancies S_v. Since the interstitial formation enthalpy H_i is several times bigger than the vacancy formation enthalpy H_v,[36,39] one can conclude that the interstitialcy formation Gibbs free energy, $\mathcal{G}_\mathrm{i} = H_\mathrm{i} - TS_\mathrm{i}$, should be much bigger than that for the vacancy, $\mathcal{G}_\mathrm{v} = H_\mathrm{v} - TS_\mathrm{v}$, and, therefore, the equilibrium concentration of vacancies $c_\mathrm{v} = \exp(-\mathcal{G}_\mathrm{v}/k_\mathrm{B}T)$ is much larger than the interstitial concentration $c_\mathrm{i} = \exp(-\mathcal{G}_\mathrm{i}/k_\mathrm{B}T)$, where k_B is Boltzmann's constant. It was concluded that there should be nearly no interstitials in thermal equilibrium. This is in line with famous experiments by Simmons and Balluffi,[45,46] who first showed that vacancies are the dominating defects in metals at high temperatures. Nowadays, this conclusion is also said to be valid and even modern textbooks often state that interstitial atoms essentially do not occur in thermodynamic equilibrium.[47] However, there are fairly strong evidences that this might be not the case as discussed below.

2.2. Effect of vacancies and interstitials on the elastic moduli

Even if interstitials cannot be produced by thermal activation, they can be created by irradiation. Aside from the aforementioned computer modeling by Gibson *et al.*[32] and Erginsoy *et al.*,[33] a solid experimental evidence for this was presented by Holder *et al.*[48,49] and Rehn *et al.*[50] They performed irradiation of copper single crystals at $T = 4$ K by thermal neutrons and simultaneously measured all 4 elastic moduli. Soft neutron irradiation produces isolated Frenkel pairs (vacancy + interstitial), which lead to a change of elastic moduli. The low temperature provided the small mobility of interstitials, which can otherwise be annihilated with vacancies. The basic result of their experiments is presented in Fig. 2. It is seen that both bulk modulus B and shear modulus C_{44} decrease with the irradiation dose but C_{44} falls much faster. This is referred to as the diaelastic effect. The magnitude, anisotropy, and temperature dependences of the elastic constants provided clear evidence for $\langle 100 \rangle$ split configuration of interstitials, which are responsible for a strong C_{44} decrease.[48] Similar experiments with close results were later performed on Al single crystals subjected to electron irradiation at $T = 4$ K.[51]

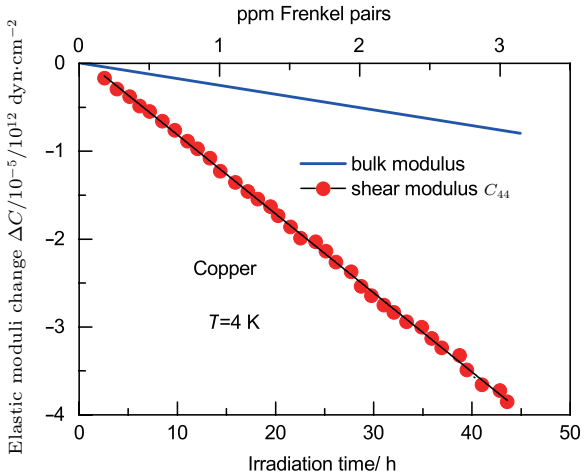


Fig. 2. (color online) Effects of low-temperature thermal neutron irradiation on the bulk and shear moduli of copper single crystals.[49,50]

The fractional decrease of the shear modulus C_{44} with defect concentration growth can be expressed as

$$\frac{\Delta C_{44}}{C_{44}} = \frac{\Delta C_{44}^{\mathrm{i}} + \Delta C_{44}^{\mathrm{v}}}{C_{44}} = -\beta_\mathrm{i} c_\mathrm{i} - \beta_\mathrm{v} c_\mathrm{v}, \tag{1}$$

where $\Delta C_{44}^{\mathrm{i}}$ and $\Delta C_{44}^{\mathrm{v}}$ are the changes of the shear modulus due to interstitialcies and vacancies in the concentrations c_i

and c_v, respectively, β_i and β_v are the corresponding dimensionless constants called the shear susceptibilities. The interstitialcy influence on the shear modulus is very large, $\beta_i = 31$ and 27 ± 2 for copper and aluminum, correspondingly, compared with $\beta_v = 2$ for vacancies (for Al).[37,49,52]

While the data shown in Fig. 2 are taken at defect concentrations of a few ppm (see the top axis), the extrapolation of C_{44} towards large concentrations leads to the conclusion that if it would be somehow possible to introduce 2% to 3% of interstitials into the crystal, the shear modulus would become zero. Meanwhile, zero shear modulus is believed to be a signature of a liquid.[53] Perhaps this was the first fact, which led Granato to make the hypothesis that melting is intimately related to dumbbell interstitials as discussed below.

2.3. Interstitial low-frequency resonance vibration modes

An important feature of dumbbell interstitials consists in the presence of low frequencies in their vibration spectrum occurring due to their high effective mass. These frequencies are several times smaller than the Debye frequency ω_D. The first experimental evidence for that was obtained in the aforementioned work by Holder *et al.*[48,49] and Rehn *et al.*,[50] who observed a strong temperature dependence of the elastic constants of irradiated Cu. The analysis of this effect showed that it originates from the resonant mode with the frequency $\omega_R = \omega_D/9$. The existence of resonant modes was confirmed by later experimental work[35,41] as well as by theoretical calculations by Dederichs *et al.*,[54,55] which arrived at a few resonant frequencies near $\omega_R \approx \omega_D/7$. These calculations showed that resonant modes always lead to large and negative changes of the shear modulus (the diaelastic effect), as found experimentally (Fig. 2). The external shear stress brings into string-like motion about two tens of atoms around the interstitalcy core (see Fig. 1(d)) leading to a strong anelastic shear modulus decrease. The second crucial point is that because of these low-frequency vibration modes, the interstitialcy formation entropy S_i becomes positive and large, several times bigger than that of the vacancy. For instance, for copper, $S_i/k_B \approx 15$ while for vacancies $S_v/k_B \approx 2.4$.[56]

Besides that, the high interstitialcy formation entropy means that its formation Gibbs free energy, $\mathcal{G}_i = H_i - TS_i$, in spite of bigger formation enthalpy H_i, can be comparable to the formation Gibbs free energy of the vacancy $\mathcal{G}_v$. Therefore, the interstitialcy concentration $c_i = \exp(-\mathcal{G}_i/k_BT)$ at high enough temperatures could be significant and should not be neglected, contrary to what usually assumed in the literature.[57] This has direct implication to the melting problem as discussed below.

Thus, the investigations performed in the 70s of the past century showed that interstitials in simple metals have the split dumbbell configuration. They (i) produce strong anelastic decrease of the shear modulus and (ii) have high formation entropy. The ITCM is intrinsically based on these two properties of the interstitialcy defect.

3. Interstitialcy theory of condensed matter states and its implication to melting and liquid state

The theory was published in 1992[58] and its simplified version was presented later in Ref. [59]. Granato calculated the Gibbs free energy of a crystal containing interstitialcies. The basic assumption of the theory consists in the hypothesis that the change of the internal energy U of a crystal with respect to the change of the intertisialcy concentration dc_i can be accepted as

$$\frac{dU}{dc_i} = \alpha_1 G(c_i)\Omega + \alpha_2 B\Omega, \tag{2}$$

where G is the shear modulus, which is dependent on c_i, B is the bulk modulus (rather insensitive to c_i), α_1 and α_2 are dimensionless constants, and Ω is the volume per atom. Granato argued that the shear energy in Eq. (2) is dominant so that the second term related to the dilatational energy can be neglected. This agrees with a general theoretical result[60] that the elastic energy of a point defect far from it is mainly the shear elastic energy, which is controlled by the shear modulus. A fit for the data taken on copper showed that $\alpha_1 \approx 1$. For clarity, we omit the subscript 1 thereafter. Granato showed that the lattice periodicity implies that the shear modulus in terms of the interstitialcy concentration can be written as

$$G = G_0 \exp(-\alpha\beta_i c_i), \tag{3}$$

where $\alpha = \frac{1}{G\Omega}\frac{dU}{dc_i}$ is the same as the above, G_0 is the shear modulus of the defectless crystal and β_i is the interstitialcy shear susceptibility (see Eq. (1)), which was theoretically estimated to be $\beta_i = 4\pi^2 \approx 40$.[58] For small c_i, equation (3) can be expanded into series as $\Delta G/G_0 = -\beta_i c_i$, where $\Delta G = G - G_0$. It is seen that this equation gives a linear decrease of the shear modulus with c_i, in line with the experimental results (Fig. 2). The theoretical and experimental β values are also comparable (≈ 40 and ≈ 30, respectively). Equation (3) may be considered as the basic equation of the ITCM.

The entropy of a crystal with interstitialcies is given by a usual configurational term (similar to that for the vacancy) and a large vibrational term determined by the resonant vibration modes. Granato then estimated the change of the vibration frequencies with increasing c_i by assuming that interstitialcies are string-like entities and derived the Gibbs free energy difference $\Delta\mathcal{G}$ as a function of c_i and T. The results in normalized dimensionless quantities at different values of the normalized temperature T/T_m (T_m is the melting temperature) are reproduced in Fig. 3. Calculation parameters were taken for copper.

It was found that different equilibrium and metastable thermodynamic states are possible depending on T/T_m.

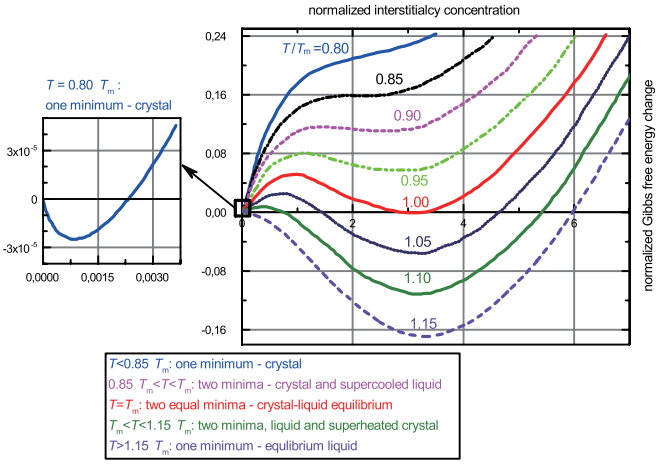


Fig. 3. Changes of the normalized Gibbs free energy with the normalized interstitialcy concentration at different values of the normalized temperature T/T_m. The legend shows that depending on T/T_m, different thermodynamic states are possible: equilibrium crystal, supercooled liquid, equilibrium liquid and superheated crystal.[58] The inset shows the Gibbs free energy minimum for $T = 0.80\ T_m$.

At $T/T_m < 0.85$, the $\Delta\mathcal{G}$ curve has only one minimum, which corresponds to the equilibrium crystalline state with certain small c_i as shown in the inset. In the range $0.85T_m < T < T_m$, the $\Delta\mathcal{G}$ curve has two minima, a deep one at a small c_i (not shown in Fig. 3) and a shallow one at a high c_i. The first $\Delta\mathcal{G}$ minimum corresponds to the equilibrium crystalline state while the second one is believed to be responsible for the metastable supercooled liquid state. At $T = T_m$ both $\Delta\mathcal{G}$ and $\frac{\partial\Delta\mathcal{G}}{\partial T}$ are zero and the $\Delta\mathcal{G}$ curve has two equal minima corresponding to the thermodynamic equilibrium between the crystalline and liquid states at small and high c_i, respectively. In the range $T_m < T < 1.15\ T_m$ there are one shallow minimum at small c_i (not shown in Fig. 3) and the second deep minimum at high concentrations, which are explained as corresponding to the metastable superheated crystal and equilibrium liquid state. Finally, at $T/T_m > 1.15$ there is only one $\Delta\mathcal{G}$-minimum at high c_i, which reflects the equilibrium liquid state.

Thus, depending on temperature and interstitialcy concentration, which in some sense can be considered as a configurational coordinate, the ITCM predicts equilibrium and metastable crystalline and liquid states. Although calculation parameters were taken for a particular metal and the theory contains certain assumptions and approximations, it makes a number of testable predictions. The most important one is that melting is related to a rapid interstitialcy generation. The primary reason for that lies in the large interstitialcy formation entropy S_i related to their resonant vibration modes. To our knowledge, the literature gives the data on the interstialcy formation entropy (in S_i/k_B units) only for Cu (15 ± 2[41,56]), Al (22[52,57]) and solid Kr (16[61]). These large S_i-values confirm the basic assumptions of the ITCM. On the other hand, it is the high S_i, which allows explaining the melting entropy known to be $\approx 1.2k_B$ per particle for all elemental substances over the Periodic Table with only a few exceptions (so-called Richards rule).[62,63]

The vibration entropy decreases at high c_i because of the interactions between interstitialcies, which reduce their vibration amplitude and increase the vibrational frequencies, leading to a decrease of the entropy. This provides the second minimum representing the liquid state.[59] Computer modeling showed that interstitials retain their individuality in the liquid.[64] Granato estimates the interstitialcy concentration in liquid Cu to be about 9%.[58] For aluminum, $S_i/k_B = 22$ and the melting entropy per atom $\Delta S_m/k_B = 1.38$. Then, one arrives at $c_i = \Delta S_m/S_i \approx 0.063$ at $T = T_m$, which is comparable to Granato's estimate for Cu. Next, using the basic equation of the ITCM (3) with the shear susceptibility for Al $\beta = 27$ and accepting $\alpha \approx 1$, one can estimate the reduction of the shear modulus of liquid aluminum at the melting point to be $G/G_0 = 0.183$. This is in good agreement with computer simulation,[65] which gives $G/G_0 = 0.163$ at $T = T_m$ for Al. The shear modulus of liquid is small but non-zero and this fact is naturally explained by the ITCM.

It is not the goal of the present work to compare the ITCM with other melting theories and we just mention a few basic facts supporting it. First, an important role of interstitialcies in melting was repeatedly mentioned in the literature (e.g., Refs. [66]–[69]). Since the shear modulus is exponentially dependent on the interstitialcy concentration (Eq. (3)), precise G-measurements can be used to monitor c_i. This was first used by Gordon and Granato[52] who arrived at the conclusion that c_i in Al is about 10^{-4}, just by an order of magnitude smaller than the vacancy concentration. This conclusion was recently confirmed by more precise measurements of G in aluminum near T_m,[57] showing that the interstitialcy Gibbs formation energy $\mathcal{G}_i$ starts to rapidly fall just below T_m promoting fast increase of c_i, which becomes only 2–3 times smaller than c_v. This also agrees with the computer simulation of Cu,[64] which revealed a decrease of the interstitialcy formation enthalpy from 3.2 eV at small c_i to 1.0 eV at $c_i = 0.03$. The assumption that the liquid contains a few percent of interstitialcy defects provides an explanation of the empirical Lindemann melting rule and a correlation between the melting temperature and shear modulus,[70] heat capacities of supercooled and equilibrium liquids,[62] famous Vogel–Fulcher–Tammann relation for the viscosity of supercooled liquids[71] as well as the fragility of liquid and its relation to the heat capacity jump at the glass transition.[62,63]

It is also worthy of notice that relatively large c_i should provide an additional contribution to the heat capacity C_p at hight temperatures. It was recently shown that this contribution in Al is indeed observed as non-linear C_p growth, which is common to simple metals and remained unexplained so far.[72]

4. Properties of metallic glasses within the framework of the ITCM

4.1. Basic assumptions of the ITCM for the glassy state

If melting is generically related to rapid multiplication of interstitialcies and they indeed exist in the liquid as identifiable structural units (but not as "defects" in the usual understanding of this term) as argued by the ITCM and supported by computer modelling, it is reasonable to assume that some part of them becomes frozen in solid glass as a result of melt quenching. Then, the properties of glass should be related to the interstitialcy defect concentration. First of all, this concerns the shear modulus of glass G. Following the logic of the ITCM, one should assume that G exponentially decreases with the interstitialcy concentration $c_i = c$ with respect to the defectless ground state. For the latter, the crystalline maternal state (which was used for glass production) with the shear modulus μ should be accepted. Then, equation (3) should be rewritten as

$$G(c) = \mu \exp(-\alpha\beta c). \tag{4}$$

This equation constitutes the first basic assumption used to describe experimental data on metallic glasses.

As mentioned above and argued below, the dilatational contribution to the internal energy is not significant. Therefore, using Eq. (2) for the case of constant pressure one can accept the interstitalcy formation enthalpy in the form

$$H(c) = \alpha G(c)\Omega, \tag{5}$$

where $G(c)$ is given by Eq. (4). The relationship (5) constitutes the second basic assumption of the ITCM as applied to the glassy state. No other major assumptions are made to explain the experimental data as discussed below (see Ref. [73]).

4.2. Structural identication of interstitialcies

Granato gave a simple one-dimensional representation of the interstitialcy defect, which is shown in Fig. 4. In a regular defectless crystal, the atoms are located in the minima of the interatomic potential (Fig. 4(a), open circles). The interstitialcy in a crystal represents two atoms sharing the same potential well (Fig. 4(a), solid circles). A similar picture can be easily envisioned in a non-crystalline structure with an irregular potential (Fig. 4(b)). For an alloy, atom displacements should be changed slightly, but the topological pattern is expected to be the same.[59,74] However, while this one-dimensional picture is fully clear, its practical importance for defect identification in three-dimensional structures is limited.

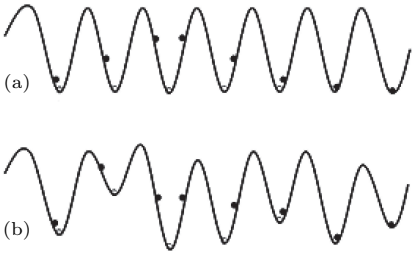


Fig. 4. Schematic drawing of the interstitialcy defect in a crystalline (a) and non-crystalline (b) structure. In both cases, the interstialcy represents two atoms sharing the same potential well.[59,74]

On the other hand, it is widely believed that equilibrium and supercooled liquids contain nanometer-scale atomic clusters of excessively high or low mobility, which are called "dynamical heterogeneities" or "cooperatively rearranging regions".[75,76] A closely related notion considers "string atoms" ("string-like solitons"[69]) repeatedly noticed in computer simulations of liquids and glasses[77,78] and said to resemble the signatures of interstitialcies in crystals.[78,79] The issue whether "strings" are related to interstitialcies was systematically tested in Ref. [64]. The authors showed that with increasing c_i the properties of interstitial atoms in computer model of crystalline copper approach and eventually completely match the properties of string atoms in the liquid. They concluded that in terms of the ITCM, the strings are direct manifestations of interstitials.

For the defect identification in the solid glassy state, it is necessary to use low temperatures because thermal activation can change the structure. In this case, other identification methods must be applied. Calculation of the vibrational density of states in molecular dynamic model of glassy copper showed that some atoms have pronounced low-frequency peaks, similar to those in the crystalline state containing interstitialcy defects.[80] It was suggested that the detection of such modes could constitute a method of identifying interstitalcy-type defects in non-crystalline structures. A later study[81,82] revealed the defects (elastic dipoles) in glassy copper with the properties similar to those of split interstitials in crystalline Cu. Thus, interstitialcy-type defects can be found in monoatomic glassy structures. Polyatomic substances are on the agenda.

4.3. Shear modulus relaxation and activation energy spectra

Since the unrelaxed shear modulus G is uniquely related to the interstitialcy defect concentration c, shear modulus of the maternal crystal μ and interstitialcy formation enthalpy H (Eqs. (4) and (5)), it actually represents the central physical quantity of the ITCM. It is important, therefore, to investigate its changes upon structural relaxation and crystallization.

First, it should be noticed that the shear modulus of as-cast metallic glass is reduced decreased by 20% to 40 % with respect to the maternal crystalline state and, correspondingly, the ratio G/μ is from 0.6 to 0.8. Then, using Eq. (4) with a

typical $\beta = 20$ and assuming $\alpha = 1$, one estimates that the initial metallic glass should contain 1.1% to 2.6% of frozen-in interstitialcy defects.

It is long known that structural relaxation of metallic glass implies a continuous distribution of underlying activation energies E.[83,84] A convenient way to analyze structural relaxation is to use the characteristic activation energy E_0, which corresponds to the maximal relaxation rate at a given instant and temperature. Then, if $n_0(E)$ is the initial interstitialcy concentration per unit activation energy interval (i.e., the initial activation energy spectrum, AES), then the relaxation is determined by the product $n_0(E)\Theta(E,T,t)$, where the function $\Theta(E,T,t)$ to a good precision can be approximated by the Heaviside step function, which is equal to 0 for activation energies $E < E_0$ and 1 for $E > E_0$.[83,84] At a constant temperature T, the characteristic activation energy $E_0 = k_B T \ln \nu t$, while upon linear heating $E_0 = AT$, where $A \approx 3.1 \times 10^{-3}$ eV/K, weakly depending on the choice of the attempt frequency ν and heating rate $\dot{T}$.[85] Then, using Eq. (4), one can arrive at the isothermal relaxation kinetics for the change of the normalized shear modulus as[86]

$$g(t) = G(t)/G_0 - 1 = \beta k_B T n_0 \ln(1 + t/\tau), \qquad (6)$$

where $G_0 = G(t = 0)$, τ is the effective preannealing time and n_0 to a good precision can be considered as a constant at $T = \text{const}$. Equation (6) gives an excellent description of the whole relaxation kinetics including a linear increase of the shear modulus with the logarithm of time after some transient defined by the condition $t \gg \tau$.[86] It is the "lnt"-kinetics, which is observed experimentally in as-cast metallic glasses.[83,84,87,88]

Using the shear modulus measurements performed at a constant heating rate in the as-cast and relaxed states, one can derive the underlying AES as[89]

$$n_0(E_0) = \beta^{-1} \frac{\mathrm{d}}{\mathrm{d}E_0} \ln \frac{G(E_0)}{G_{\mathrm{rel}}(E_0)}, \qquad (7)$$

where the functions $G(E_0)$ and $G_{\mathrm{rel}}(E_0)$ can be determined from temperature depedences $G(T)$ and $G_{\mathrm{rel}}(T)$. A typical example of the AES thus obtained is given in Fig. 5. The low- and high-energy parts of the AES ($E_0 < 1.3$ eV and $E_0 > 2.2$ eV, respectively) correspond to the beginning and end of structural relaxation below T_g. Integration of the AES allows calculating the change of the absolute interstitialcy defect concentration upon structural relaxation, $\Delta c = \int n_0(E_0)\mathrm{d}E_0$. For the data shown in Fig. 5, one obtains $\Delta c = 0.0023$. Similar Δc-data were obtained for other metallic glasses, see Table 1 below.[90] Comparing these values with the estimates of the full interstitialcy concentration given above, one can conclude that only about one tenth of frozen-in defects can be annealed out during structural relaxation. Further decrease of c down to zero is related to crystallization as discussed below.

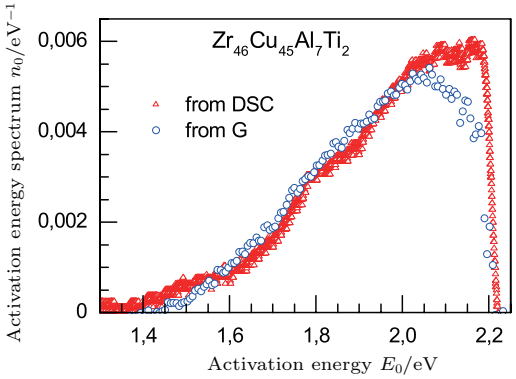


Fig. 5. (color online) Activation energy spectra of structural relaxation of a Zr-based bulk glass derived from shear modulus relaxation and calorimetric data.[90] With a permission from Elsevier.

4.4. Evolution of the shear modulus upon linear heating

A typical pattern showing the evolution of the shear modulus of a metallic glass upon linear heating into the glass transition region and cooling back to room temperature is given in Fig. 6. A general trend consists in a decrease of G with temperature, which becomes much faster in the T_g region. Cooling from above T_g leads to a big hysteresis so that G increases by $\approx 4\%$ as a result of the whole heating→cooling cycle. The G-changes upon heating and cooling contain both instantaneous anharmonic and time-dependent relaxation components. On the other hand, red squares in Fig. 6 give temperature dependence of the shear modulus in the metastable equilibrium obtained by long-term isothermal annealing.[91] It is seen that the relaxation takes place always towards the metastable equilibrium. The relaxation component can be separated as shown by solid blue circles in Fig. 7. Then, using Eq. (4) and assuming that the activation energy of elementary shear rearrangements is proportional to the shear modulus, a differential equation for the relaxation component based on the ITCM approach can be written down and solved.[92] The solution is given in Fig. 7.

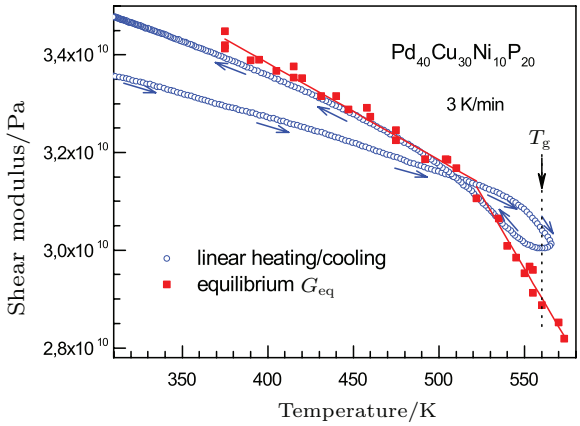


Fig. 6. (color online) Temperature changes of the shear modulus of bulk glassy $Pd_{40}Cu_{30}Ni_{10}P_{20}$ upon heating into the glass transition region and subsequent cooling. Red squares represent the temperature dependence of the shear modulus in the metastable equilibrium derived isothermally.[91,92]

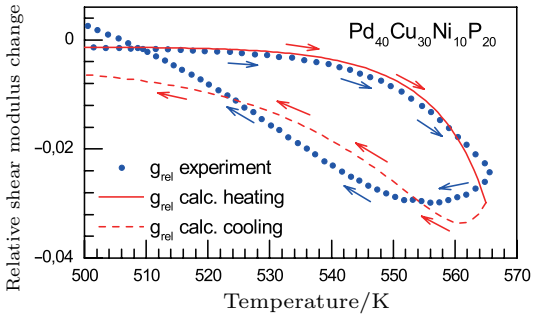


Fig. 7.(color online) Relaxation component (solid blue circles) of the shear modulus of bulk glassy $Pd_{40}Cu_{30}Ni_{10}P_{20}$ derived using the data shown in Fig. 6. Solid and dash red curves give the solution of the differential equation for the relaxation.[92] With a permission from Elsevier.

It is seen that the calculation reproduces the experimental result quite reasonably. An increase (decrease) of the shear modulus towards metastable equilibrium is due to a decrease (increase) of the interstitialcy defect concentration. Respectively, a sharp drop of the derivative $\mathrm{d}G/\mathrm{d}T$ slightly below T_g reported for all studied metallic glasses[89,91,93,94] is actually a consequence of the increased relaxation rate towards the metastable equilibrium. Similar results were obtained for the shear modulus data derived at different heating rates.[95]

4.5. Relation between the shear moduli of glass and maternal crystal

Equation (4) imposes certain restrictions on the shear moduli of glass G and maternal crystal μ and their temperature dependences. Indeed, this relationship can be rearranged as

$$\frac{\mathrm{d}}{\mathrm{d}T}\ln\frac{\mu(T)}{G(T)} = \alpha\beta\frac{\mathrm{d}c}{\mathrm{d}T}. \tag{8}$$

Equation (8) shows that if structural relaxation is absent and, therefore, $c = \text{const}$, then the term on its left-hand side should be zero, resulting in the equality $\frac{1}{G}\frac{\mathrm{d}G}{\mathrm{d}T} = \frac{1}{\mu}\frac{\mathrm{d}\mu}{\mathrm{d}T}$. The latter relation means that the temperature coefficients of the shear moduli in the glassy and crystalline states should be equal. On the other hand, structural relaxation far below the glass transition temperature T_g leads to an increase of the shear modulus G and, according to Eq. (4), the defect concentration c should decrease. According to Eq. (5), this should result in a release of the enthalpy and related exothermal heat flow. On the contrary, structural relaxation in the glass transition region above T_g reduces G because of a c-increase and, in line with Eq. (5), the enthalpy should be absorbed, resulting in endothermal heat flow. Consequently, negative or positive change of the derivative $\frac{1}{G}\frac{\mathrm{d}G}{\mathrm{d}T}$ related to exothermal or endothermal heat reactions should be observed. A verification of these predictions can be performed with the data shown in Fig. 8, which were taken on a Zr-based glass in the initial and relaxed states. It is seen that, indeed, that the derivative $\frac{\mathrm{d}}{\mathrm{d}T}\ln\frac{\mu(T)}{G(T)} = 0$ below $T \approx 440$ K, where structural relaxation is absent. At higher temperatures, this derivative becomes first negative (in the range corresponding to the exothermal structural relaxation-induced heat flow below T_g) and then positive (upon approaching T_g with related endothermal heat effect).[96] It was also found that the temperature coefficients of G in the relaxed glassy state (in the absence of structural relaxation) and μ in the crystalline state are equal,[73] in line with the above prediction. The same results were obtained for a Pd-based metallic glass.[89]

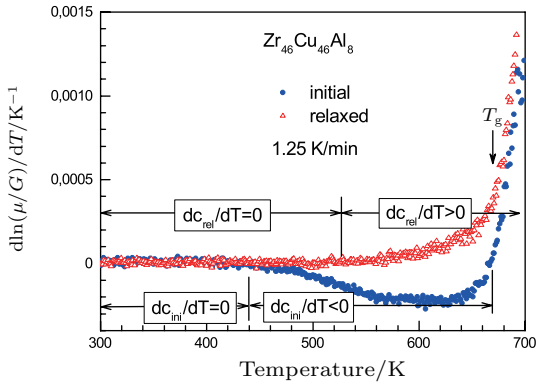


Fig. 8 (color online) Verification of Eq. (8) using shear modulus data taken on a Zr-based metallic glass in the initial and relaxed states.[96]

4.6. Effect of high-temperature annealing on room-temperature shear modulus

Kahl *et al.*[97] performed a detailed study of the effect of structural relaxation on the shear modulus of bulk glassy $Pd_{40}Ni_{40}P_{20}$. They subjected the samples to different annealing paths, quenched them into water and then measured room temperature shear modulus G^{rt}. Their results are shown by different symbols in Fig. 9. It is seen that the annealing of sample at subsequently increasing annealing temperatures T_a results, first, in a gradual increase of G^{rt} and, next, at $T_a > T_g$, in its rapid decrease (red solid circles). Subsequent long time annealing below T_g leads to an increase of G^{rt} with T_a decreasing.

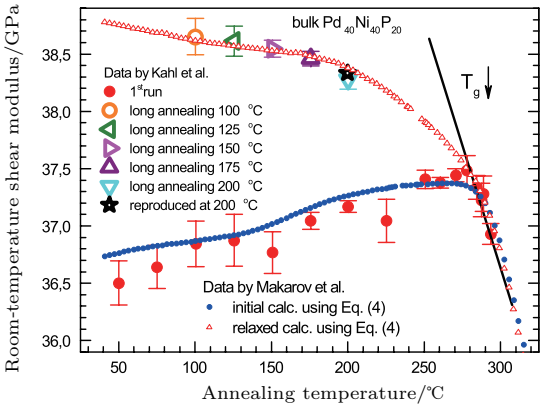


Fig. 9. (color online) Room-temperature shear modulus of bulk glassy $Pd_{40}Ni_{40}P_{20}$ after different isothermal annealing paths[97]) and calculated from Eq. (4) using linear heating shear modulus data for the initial, relaxed and crystalline states shown in Fig. 10(a) and temperature dependence of the interstitialcy defect concentration given in Fig. 10(b).[94] With a permission from Elsevier.

In spite of rather complicated $G^{rt}(T_a)$ pattern given in Fig. 9, it can be readily explained by Eq. (4).[98] For this, temperature dependence of the interstitialcy defect concentration should be determined from independent shear modulus measurements on the same glass. The corresponding shear modulus data for the initial state (run 1) and after heating above T_g (relaxed state, run 2) together with the data for fully crystallized state were reported in Ref. [94] and are shown in Fig. 10(a). These data can be next used for calculating the interstitialcy defect concentration using Eq. (4). The result, which is typical, is given in Fig. 10(b). It is seen that the defect concentration in the initial state first slightly decreases with temperature increasing and rapidly increases above T_g after that. In the relaxed state (run 2), c gradually increases with temperature increasing at $T < T_g$ that next transforms into a rapid defect multiplication above T_g. Now, we consider the fact that the sample is quenched from any temperature T_a in Fig. 10(b) to room temperature at infinitely large rate. Then, the defect concentration at room temperature remains exactly the same and the shear modulus becomes $G^{rt} = \mu^{rt} \exp[-\beta c(T_a)]$, where μ^{rt} is room-temperature shear modulus of the maternal crystal. The $G^{rt}(T_a)$ dependence thus calculated is shown in Fig. 9 by the same symbols, which were used in Fig. 10(b) for $c(T)$ dependences. It is seen that the calculation gives an excellent reproduction of Kahl *et al.*'s data. This calculation, again, provides a clear support for the relationship between the shear moduli of glass and maternal crystal given by Eq. (4).

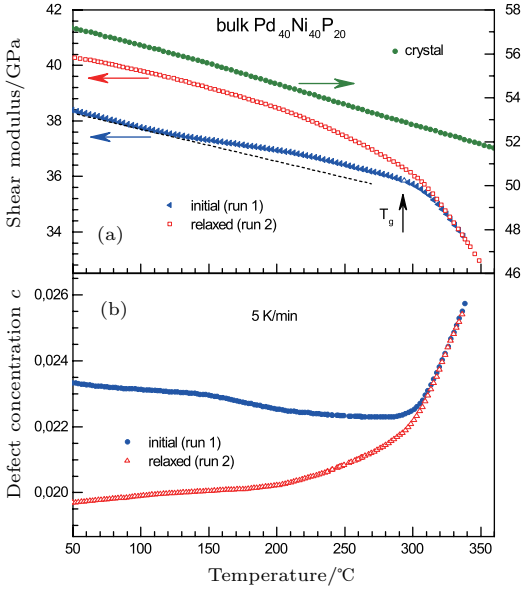


Fig. 10. (color online) (a) Temperature dependences of the shear modulus of glassy $Pd_{40}Ni_{40}P_{20}$ in the initial state (run 1), after heating into the supercooled liquid region (run 2) and after full crystallization. (b) Interstitialcy defect concentration calculated from Eq. (4).[94] With a permission from Elsevier.

4.7. Heat effects due to structural relaxation and crystallization of metallic glasses

According to Eq. (4), a change of the interstitialcy defect concentration c leads to the alteration of the shear modulus G. In turn, a change of G varies the enthalpy (heat content) H as supposed by Eq. (5). It is evident, therefore, that all relaxation phenomena in glass should be intrinsically related to heat effects.

Heat effects in metallic glasses are most often studied by the differential scanning calorimetry (DSC), which measures the heat flow per unit mass W. Combining Eqs. (4) and (5), one can derive an expression for W as[99]

$$W = \frac{\dot{T}}{\beta\rho}\left[\frac{G^{rt}}{\mu^{rt}}\frac{d\mu}{dT} - \frac{dG}{dT}\right], \tag{9}$$

where ρ is the density, G^{rt} and μ^{rt} are the shear moduli at room temperature and other quantities have the same meaning as the above. It was later found that a more general form of the heat flow is[100]

$$W = \frac{\dot{T}}{\beta\rho}\left[\frac{G}{\mu}\frac{d\mu}{dT} - \frac{dG}{dT}\right], \tag{10}$$

which differs from Eq. (9) by the multiplier in front of the derivative $\frac{d\mu}{dT}$.

Equations (9) and (10) were repeatedly tested on different metallic glasses.[93,94,99–102] It was found that they both give quite a good description of the kinetics of exothermal heat flow below T_g and endothermal heat flow in the glass transition region both in the initial and relaxed glassy states. However, equation (10) provides slightly more precise description of the experiment.[100] Furthermore, rather unexpectedly, it was found that these equations give a good description of the heat flow upon crystallization. This is exemplified by Fig. 11, which gives an experimental DSC run taken on a Zr-based metallic glass together with the calculated DSC curve using Eq. (9) with the shear susceptibility $\beta = 18$.[103] It is seen that this equation gives an excellent description of the experimental heat release below T_g, heat absorption above T_g and crystallization-induced heat release. In particular, the height and temperature of crystallization heat release peak coincide with the experimental results within less than 10% and ≈ 3 K, respectively. The quality of the fit with Eq. (10) is almost the same. It is to be emphasized that Eqs. (9) and (10) actually contain no fitting parameters. The only quantity, which can be slightly varied, is β. This variation, however, is very limited since β changes within a narrow range $16 \leq \beta \leq 20$ for Zr- and Pd-based metallic glasses and only for a La-based glass $\beta = 25$ was reported.[90]

Equations (9) and (10) show that heat effects upon structural relaxation and crystallization are controlled by the shear moduli of glass and maternal crystal. This emphasizes once more the generic relationship between glass and maternal crystal.

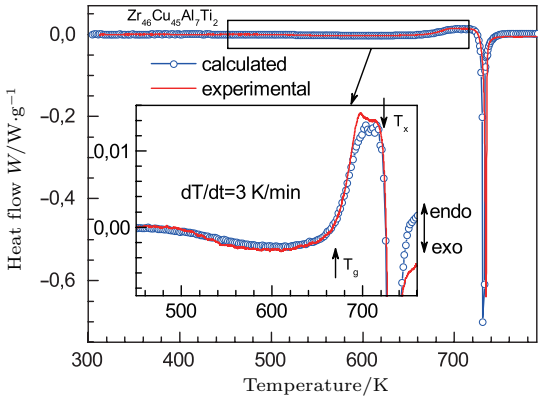


Fig. 11. (color online) Experimental DSC traces for bulk glassy $Zr_{46}Cu_{45}Al_7Ti_2$ together the heat flow calculated with Eq. (9). The inset shows the exothermal flow below T_g and endothermal flow in the suppercooled liquid state on an enlarged scale. An excellent correspondence between experimental and calculated heat flow both in the glassy state and upon crystallization is seen.[103]

The fact that equations (9) and (10) describe heat effects both in the glassy state and upon crystallization clearly indicates that the difference in the internal energy between glassy and crystalline states is determined mostly by the elastic energy related to the interstitialcy defects frozen-in upon glass production. This major hypothesis was first proposed in Ref. [104] and later tested in detail in the experiment described in Ref. [105]. The underlying idea is as follows. The difference $\rho\Delta U$ between the internal energies per unit volume of initial glass and maternal crystal within the framework of the ITCM can be calculated as[100]

$$\rho\Delta U = \frac{\mu}{\beta}\left[1-\frac{G}{\mu}\right]. \tag{11}$$

Since, as already mentioned above, the volume change occurring upon crystallization of glass gives an insignificant contribution to the change of the internal energy (see also Refs. [93], [100], and [104]), the above difference $\rho\Delta U$ should be treated as the heat of crystallization per unit volume, i.e., $\rho\Delta U = \rho Q_{\rm cr}$, where $Q_{\rm cr}$ is the heat of crystallization. The experiment[105] consisted in the measurement of the shear modulus change just upon crystallization and the determination of the corresponding crystallization heat $Q_{\rm cr}$. The result of this experiment is given in Fig. 12, which shows that $\rho\Delta U$ linearly increases with increasing $\rho Q_{\rm cr}$. The dash line in this figure gives the unity slope line drawn through the origin. This line almost coincides with the linear least-square fit calculated over all data points. Thus, the data in Fig. 12 provide compelling evidence that indeed $\rho\Delta U \approx \rho Q_{\rm cr}$ and, therefore, the heat of crystallization is determined by the dissipation of the elastic energy related to the system of interstitialcy defects frozen in glass upon melt quenching.[105]

It is also worthy noting that equations (9) and (10) for the heat flow allow the reconstruction of the activation energy spectrum responsible for structural relaxation using calorimetric measurements. The corresponding calculation for the AES yields[106]

$$n_0(E_0) = \frac{\rho}{\dot{T}AG^{\rm rt}}\Delta W(E_0), \tag{12}$$

where $\Delta W = W_{\rm rel} - W$ with W and $W_{\rm rel}$ being the heat flows in the initial state and relaxed state obtained by heating into the supercooled liquid region, respectively. All other quantities have the same meanings as the above (see Eq. (7) and relevant explanation). An example of AES reconstruction with Eq. (12) is given in Fig. 5 together with the AES derived by using shear modulus relaxation data with Eq. (7). It is seen that the two independent methods of AES reconstruction by using shear modulus and calorimetric data give practically the same result. This further indicates the self-consistency of the ITCM and again emphasizes the generic relationship between the shear elasticity and heat effects in metallic glasses. As mentioned above, this relationship is based on the two basic assumptions of the ITCM given by Eqs. (4) and (5).

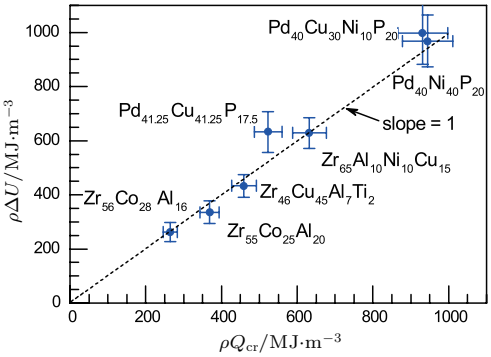


Fig. 12. (color online) Crystallization-induced change of the internal energy per unit volume $\rho\Delta U$ calculated using Eq. (11) as a function of the crystallization heat per unit volume $\rho Q_{\rm cr}$ for Pd- and Zr-based metallic glasses.[105] With a permission from Elsevier.

4.8. Formation enthalpy of interstitialcy defects

There is an interesting way to determine the formation enthalpy of defects responsible for structural relaxation of metallic glasses.[90,106] On the one hand, if these defects are actually interstitialcies, their formation enthalpy can be calculated within the framework of the ITCM using Eq. (5). One the other hand, the same quantity can be derived from shear modulus and DSC data as follows. First, one can derive the activation energy spectrum $n_0(E_0)$ using Eq. (7) or (12). Next, one can determine the change of the defect concentration by integration over the AES, i.e., $\Delta c = \int n_0(E_0)\mathrm{d}E_0$. This allows calculating the absolute number of defects per mole annealed out during structural relaxation $\Delta N_\mu = \Delta c N_{\rm A}$ with $N_{\rm A}$ being the Avogadro number. Then, one can derive the heat of structural relaxation $Q_{\rm sr} = \int [W(t) - W_{\rm rel}(t)]\,\mathrm{d}t$, where W and $W_{\rm rel}$ are the heat flows in the initial and relaxed states, respectively. Finally, one can calculate the heat release per defect $Q_{\rm d} = Q_{\rm sr}/N_\mu$, which actually constitutes the "experimental" defect formation enthalpy. This algorithm was implemented in Refs. [90] and [106] and the results for different metallic glasses are summarized in Table 1, which gives the quantities

Δc, N_μ, Q_d, and H (calculated using Eq. (5) with $\alpha = 1$). It is seen that in all cases the "experimental" defect formation enthalpy is very close to the interstitialcy formation enthalpy determined from Eq. (5). This gives another independent confirmation of the idea that the defects annealing out upon structural relaxation are indeed interstialcies.

Table 1. Parameters of structural relaxation of metallic glasses: change of the defect concentration Δc, number of annealed defects per mole N_μ, heat of structural relaxation per defect Q_d, and interstitialcy formation enthalpy H.[90] With a permission from Elsevier.

Glass	Δc	$N_\mu/10^{20}$ mole^{-1}	Q_d/eV	H/eV
$La_{55}Al_{25}Co_{20}$	0.00246	14.8	2.65	2.63
$Zr_{46}Cu_{46}Al_8$	0.00215	13.0	3.79	3.69
$Zr_{46}Cu_{45}Al_7Ti_2$	0.00230	13.9	3.66	3.63
$Zr_{56}Co_{28}Al_{16}$	0.00238	14.3	4.07	3.89
$Pd_{40}Ni_{40}P_{20}$	0.00318	19.2	3.04	3.08
$Pd_{41.25}Cu_{41.25}P_{17.5}$	0.00170	10.3	2.63	2.73
$Pd_{40}Cu_{30}Ni_{10}P_{20}$	0.00208	14.1	2.85	2.77

5. Conclusions

The Interstitialcy theory of condensed matter (ITCM) states argues that the basic defect responsible for the diaelasticity and related phenomena in crystalline metals is the interstitial in the split dumbbell configuration (interstitialcy), which is found in different crystalline lattices. Due to a specific structure of the defect, it has low frequency vibration modes, which define a large formation entropy S_i. The applied shear stress brings into string-like motion several tens of atoms around the defect nuclei defining a strong anelastic decrease of the shear modulus G. Large vibration entropy and strong shear susceptibility are the major properties of the interstitialcy distinguishing it from the vacancy.

The ITCM considers that approaching to the melting temperature results, due to the large S_i, in a rapid decrease of the interstitialcy formation Gibbs free energy $\mathcal{G}_i = H_i - TS_i$, which leads to an increase of the interstitialcy concentration c_i. The latter, in turn, reduces the interstitialcy formation enthalpy H_i that also favours the decrease of $\mathcal{G}_i$ and again results in an increase of c_i. Eventually, the crystal looses the shear stability and melts. The thermodynamic analysis shows that depending on temperature and interstitialcy concentration, several thertmodynamic states are possible: equilibrium crystal, superheated crystal, equilibrium liquid and supercooled liquid.

In the liquid state, interstitalcies do not loose their identity being now inherent structural elements rather than defects in the usual understanding of this term. Melt quenching freezes a part of interstitialcy defects in solid glass. It is believed that these defects preserve the major properties characteristic of the original (maternal) crystalline state as supposed by equations (4) and (5). The maternal crystalline state represents the ground state allowing monitoring the absolute defect concentration. It is suggested that structural relaxation of glass is governed by the defect concentration while the crystallization heat originates from the release of the defect elastic energy.

This conceptual framework allows explaining various phenomena in metallic glasses under different experimental conditions. It contains certain assumptions, simplifications and approximations. However, it makes testable predictions, and in all cases considered so far, the ITCM provides either quite reasonable or rather exact description of the relaxation kinetics. In our opinion, it could serve as a solid basis for the understanding of the generic interconnection of the properties of metallic crystalline, liquid and glassy materials.

Due to space limitations, several important issues and their interpretation within the framework of the ITCM are omitted in this review. First of all, this concerns the role of the anharmonicity of the interatomic potential, which plays a crucial role in the shear softening and heat effects in metallic glasses.[73,93,101] We do not consider the heat release due to structural relaxation-induced dilatation,[107,108] nor the explanation of the low temperature Boson heat capacity peak within the framework of the ITCM[109] nor the elastic dipole model, which starts with the statement that interstitialcies are in fact elastic dipoles and ends up with heat and shear softening relations fully similar to those derived within the framework of the ITCM despite of fully different starting points.[93,100,105] The interested reader is referred to the corresponding original papers.

Since interstitalcies are proven to exist in different structures, including two component ones (so-called "mixed dumbbells"[41]), there is general expectation that the ITCM should be applicable not only for metallic materials but for materials with other interatomic bonding. A verification of this hypothesis constitutes a major challenge to the future research.

Acknowledgment

The present author was lucky to work in a close contact for quite a few years with Professor Andrew Vincent Granato (1926-2015), a true intellectual and talented scientist. This paper is fully based on that work and devoted to his memory. The author is also thankful to Dr. D M Joncich (University of Illinois at Urbana-Champaign, USA), Dr. N P Kobelev (Institute for Solid State Physics, Russian Academy of Sciences, Chernogolovka, Russia) and VSPU colleagues, Yu P Mitrofanov, R A Konchakov, G A Afonin, A S Makarov, and E V Safonova, for multiyear fruitful cooperation.

References

[1] Elliott S R 1984 *Physics of Amorphous Materials* (New York: Longman)
[2] Jäckle J 1986 *Rep. Prog. Phys.* **49** 171
[3] Nemilov S V 1995 *Thermodynamic and Kinetic Aspects of the Vitreous State* (Boca Raton: CRC Press)

[4] Zallen R 1998 *The Physics of Amorphous Solids* (New York, Chichester, Weinheim, Brisbane, Singapore, Toronto: John Wiley & Sons)

[5] Donth E 2001 *The Glass Transition: Relaxation Dynamics in Liquids and Disordered Materials* (Berlin, Heidelberg, New York: Springer-Verlag)

[6] Rao K J 2002 *Structural Chemistry of Glasses* (Elsevier Science & Technology Books)

[7] Dyre J C 2006 *Rev. Mod. Phys.* **78** 953

[8] Angell C A 2008 *MRS Bull.* **33** 544

[9] Schmelzer J W P and Gutzow I S 2011 *Glasses and the Glass Transition* (Weinheim: Wiley-VCH)

[10] Wolynes P G and Lubchenko V 2012 *Structural Glasses and Supercooled liquids. Theory, Experiment, and Applications* (Hoboken, New Jersey: John Wiley & Sons)

[11] Schuh C A, Hufnagel T C and Ramamurty U 2007 *Acta Mater.* **55** 4067

[12] Inoue A and Takeuchi A 2007 *Acta Mater.* **59** 2243

[13] Trexler M M and Thadhani N N 2010 *Prog. Mater. Sci.* **55** 759

[14] Wang W H 2012 *Prog. Mater. Sci.* **57** 487

[15] Egami T, Iwashita T and Dmowski W 2013 *Metals* **3** 77

[16] Yu H B, Wang W H and Samwer K 2013 *Mater. Today* **16** 183

[17] Greer A L 2014 *Metallic Glasses. In Physical Metallurgy*, vol. I, (Ed. Laughlin D E, Hono K) (Oxford, UK: Elsevier) pp. 305–385

[18] Johnson W L 2015 *Nature* **14** 553

[19] Liu C, Pineda E and Crespo D 2015 *Metals* **5** 1073

[20] Ma E 2015 *Nat. Mater.* **14** 547

[21] Sun B A and Wang W H 2015 *Prog. Mater. Sci.* **74** 211

[22] Garrett G R, Demetriou M D, Launey M E and Johnson W L 2016 *Proc. Nat. Acad. Sci.* **113** 10257

[23] Wang W H, Yang Y, Nieh T G and Liu C T 2015 *Intermetallics* **67** 81

[24] Langer J C 2007 *Physics Today* **60** 9

[25] Egami T 2010 *JOM* **62** 70

[26] Frenkel J 1926 *Z. Phys.* **35** 652

[27] Frenkel J 1937 *Trans. Faraday Soc.* **33** 58

[28] Frenkel J 1946 *Kinetic Theory of Liquids* (New York: Oxford University Press)

[29] van Bueren H G 1961 *Imperfections in Crystals* (Amsterdam: North-Holland)

[30] Damask A C and Dienes G J 1963 *Point Defects in Metals* London: Gordon and Breach

[31] Seitz F 1950 *Acta Crystallogr.* **3** 355

[32] Gibson J B, Goland A N, Milgram M and Vineyard G H 1960 *Phys. Rev.* **120** 1229

[33] Erginsoy C, Vineyard G H and Englert A 1964 *Phys. Rev.* **133** A595

[34] Schilling W 1978 *J. Nucl. Mater.* **69** 465

[35] Young F W Jr 1978 *J. Nucl. Mater.* **69** 310

[36] Ehrhart P, Robrock K H, Schober H R 1986 *Physics of Radiation Effects in Crystals* (Ed. R A Johnson, A N Orlov) Elsevier Science Publishers pp. 3–115

[37] Robrock K H 1990 *Mechanical Relaxation of Interstitials in Irradiated Metals* (Berlin: Springer-Verlag)

[38] Schilling W 1994 *J. Nucl. Mater.* **216** 45

[39] Wolfer W G 2012 *Fundamental Properties of Defects in Metals. In Comprehensive Nuclear Materials* (Ed. R J M Konings) Amsterdam: Elsevier

[40] Haubold H G and Martinsen D 1978 *J. Nucl. Mater.* **69** 644

[41] Ehrhart P 1991 *Atomic Defects in Metals* Landolt-Börnstein New Series III, vol. 25 (Ed. H Ullmaier) Berlin: Springer p. 88

[42] Morgenstern M and Michely T 1997 *Phys. Rev. Lett.* **79** 1305

[43] Granato A V 1993 *J. Non-Cryst. Sol.* **156** 402

[44] Kraftmakher Y 2000 *Lecture Notes on Equilibrium Point Defects and Thermophysical Properties of Metals* Singapore: World Scientific

[45] Simmons R O and Balluffi R W 1960 *Phys. Rev.* **117** 52

[46] Simmons R O and Balluffi R W 1963 *Phys. Rev.* **129** 1533

[47] Gottstein G 2004 *Physical Foundations of Materials Science* (Berlin: Springer)

[48] Holder J, Granato A V and Rehn L E 1974 *Phys. Rev. Lett.* **32** 1054

[49] Holder J, Granato A V and Rehn L E 1974 *Phys. Rev.* **10** 363

[50] Rehn L E, Holder J, Granato A V, Coltman R R and Young F W Jr 1974 *Phys. Rev.* **10** 349

[51] Robrock K H and Schilling W 1976 *J. Phys. F: Met. Phys.* **6** 303

[52] Gordon C A and Granato A V 2004 *Mater. Sci. Eng. A* **370** 83

[53] Born M 1939 *J. Chem. Phys.* **7** 591

[54] Dederichs P H, Lehman C and Scholz A 1973 *Phys. Rev. Lett.* **31** 1130

[55] Dederichs P H, Lehman C, Schober H R, Scholz A and Zeller R 1978 *J. Nucl. Mater.* **69** 176

[56] Nordlund K and Averback R S 1998 *Phys. Rev. Lett.* **80** 4201

[57] Safonova E V, Mitrofanov Yu P, Konchakov, Vinogradov A Yu, Kobelev N P and Khonik V A 2016 *J. Phys.: Condens. Matter* **28** 215401

[58] Granato A V 1992 *Phys. Rev. Lett.* **68** 974

[59] Granato A V 2014 *Eur. J. Phys.* **87** 18

[60] Dyre J C 2007 *Phys. Rev. B* **75** 092102

[61] Gordon C A, Granato A V and Simmons R O 1996 *J. Non-Cryst. Sol.* **205** 216

[62] Granato A V 2002 *J. Non-Cryst. Sol.* **307** 376

[63] Granato A V 2006 *J. Non-Cryst. Sol.* **352** 4821

[64] Nordlund K, Ashkenazy Y, Averback R S and Granato A V 2005 *Europhys. Lett.* **71** 625

[65] Forsblom M and Grimvall G 2005 *Nature Mater.* **4** 388

[66] Stillinger F H and Weber T A 1984 *J. Chem. Phys.* **81** 5095

[67] Lee G C S and Li J C M 1989 *Phys. Rev. B* **39** 9302

[68] Kanigel A, Adler J and Polturak E 2001 *Int. J. Mod. Phys. C* **12** 727

[69] Zhang H, Khalkhali M, Liu Q and Douglas J F 2013 *J. Chem. Phys.* **138** 12A538

[70] Granato A V, Joncich D M and Khonik V A 2010 *Appl. Phys. Lett.* **97** 171911

[71] Granato A V 2011 *J. Non-Cryst. Sol.* **357** 334

[72] Safonova E V, Konchakov R A, Mitrofanov Yu P, Vinogradov A Yu and Khonik V A 2016 *J. Exp. Theor. Phys. Lett.* **103** 765

[73] Khonik V A 2015 *Metals* **5** 504

[74] Granato A V 2009 *Mater. Sci. Eng. A* **521** 6

[75] Ediger M D 2000 *Annu. Rev. Phys. Chem.* **51** 99128

[76] Betancourt B A P, Douglas J F and Starr F W 2014 *J. Chem. Phys.* **140** 204509

[77] Donati C, Douglas J F, Kob W, Plimpton S J, Poole P H and Glotzer S C 1998 *Phys. Rev. Lett.* **80** 2338

[78] Oligschleger C and Schober H R 1999 *Phys. Rev. B* **59** 811

[79] Schober H R 2002 *J. Non Cryst. Sol.* **307** 40

[80] Konchakov R A and Khonik V A 2014 *Phys. Solid State* **56** 1368

[81] Konchakov R A, Khonik V A and Kobelev N P 2015 *Phys. Solid State* **57** 856

[82] Konchakov R A, Khonik V A, Kobelev N P and Makarov A S 2016 *Phys. Solid State* **58** 215

[83] Gibbs M R J, Evetts J E and Leake J A 1983 *J. Mater. Sci.* **18** 278

[84] Khonik V A 2000 *Phys. Stat. Sol.* **177** 173

[85] Khonik V A, Kitagawa K and Morii H 2000 *J. Appl, Phys.* **87** 8440

[86] Khonik S V, Granato A V, Joncich D M, Pompe A and Khonik V A 2008 *Phys. Rev. Lett.* **100** 065501

[87] Bothe K and Neuhäuser H 1983 *J. Non-Cryst. Sol.* **56** 279

[88] Mitrofanov Yu P, Khonik V A and Vasil'ev A N 2009 *J. Exp. Theor. Phys.* **108** 830

[89] Makarov A S, Khonik V A, Mitrofanov Yu P, Granato A V, Joncich D M and Khonik S V 2013 *Appl. Phys. Lett.* **102** 091908

[90] Mitrofanov Yu P, Wang D P, Wang W H and Khonik V A 2016 *J. Alloys Comp.* **677** 80

[91] Mitrofanov Yu P, Khonik V A, Granato A V, Joncich D M, Khonik S V and Khoviv A M 2012 *Appl. Phys. Lett.* **100** 171901

[92] Khonik V A, Mitrofanov Yu P, Makarov A S, Konchakov R A, Afonin G V and Tsyplakov A N 2015 *J. Alloys Comp.* **628** 27

[93] Kobelev N P, Khonik V A, Makarov A S, Afonin G V and Mitrofanov Yu P 2014 *J. Appl. Phys.* **115** 033513

[94] Makarov A S, Khonik V A, Wilde G, Mitrofanov Yu P and Khonik S V 2014 *Intermetallics* **44** 106

[95] Mitrofanov Yu P, Khonik V A, Granato A V, Joncich D M and Khonik S V 2011 *J. Appl. Phys.* **109** 073518

[96] Makarov A S, Mitrofanov Yu P, Afonin G V, Khonik V A and Kobelev N P 2015 *Phys. Sol. State* **57** 978

[97] Kahl A, Koeppe T, Bedorf D, Richert R, Lind M L, Demetriou M D, Johnson W L, Arnold W and Samwer K 2009 *Appl. Phys. Lett.* **95** 201903

[98] Makarov A S, Khonik V A, Mitrofanov Yu P and Tsyplakov A N 2016 *Intermetallics* **69** 10

[99] Mitrofanov Yu P, Makarov A S, Khonik V A, Granato A V, Joncich D M and Khonik S V 2012 *Appl. Phys. Lett.* **101** 131903

[100] Kobelev N P and Khonik V A 2015 *J. Non-Cryst. Sol.* **427** 184

[101] Makarov A S, Khonik V A, Mitrofanov Yu P, Granato A V and Joncich D M 2013 *J. Non-Cryst. Solids* **370** 18

[102] Tsyplakov A N, Mitrofanov Yu P, Khonik V A, Kobelev N P and Kaloyan A A 2015 *J. Alloys Comp.* **618** 449

[103] Mitrofanov Yu P, Wang D P, Makarov A S, Wang W H and Khonik V A 2016 *Sci. Rep.* **6** 23026

[104] Kobelev N P, Khonik V A, Afonin G V and Kolyvanov E L 2015 *J. Non-Cryst. Sol.* **411** 1

[105] Afonin G V, Mitrofanov Yu P, Makarov A S, Kobelev N P, Wang W H and Khonik V A 2016 *Acta Mater.* **115** 204

[106] Tsyplakov A N, Mitrofanov Yu P, Makarov A S, Afonin G V and Khonik V A 2014 *J. Appl. Phys.* **116** 123507

[107] Khonik V A and Kobelev N P 2014 *J. Appl. Phys.* **115** 093510

[108] Mitrofanov Yu P, Csach K, Juríková, Miškuf J, Wang W H and Khonik V A 2016 *J. Non-Cryst. Sol.* **448** 31

[109] Vasiliev A N, Voloshok T N, Granato A V, Joncich D M, Mitrofanov Yu P and Khonik V A 2009 *Phys. Rev. B* **80** 172102